Open Access

Iraqi Journal of Industrial Research (IJOIR)

Journal homepage: http://ijoir.gov.iq

Phy-X/PSD and NGCAL Models of Several Metal Sulphides: Theoretical Prediction of Gamma Shielding Efficiency

Nadher Ali Salman, Kafa Khalaf Hammud*

Iraqi Atomic Energy Commission, Iraq

Article information

Article history:
Received: June, 09, 2024
Accepted: August, 30, 2024
Available online: December, 14, 2024

Keywords:
Gamma shielding,
Phy-X,
NGCAL,
Gamma Protection Efficiency (GPE)

Corresponding Author:
Kafa Khalaf Hammud
kafaakhalaf@gmail.com

DOI:
https://doi.org/10.53523/ijoirVol11I3ID480

Abstract

Various metal sulphides were selected for gamma and neutron shielding prediction by (Phy-X and NGCAL). The gamma parameters calculated by both software programs in the studied energy range were found to be identical, with differences (Δ% less than 1%) between both models. The Mass Attenuation Coefficient (MAC), Mean Free Path (MFP), Half Value Layer (HVL), Tenth Value Layer (TVL), and Effective Atomic Number (Z_{eff}) were calculated. Ag_2S was a superior neutron and photon attenuator because it contains two silver ions with the highest density, mean atomic number, and metal composition in addition to the lowest (S%) among all sulphides under evaluation. Additionally, the Ag_2S monoclinic network is fabricated from ($2Ag^+$) linked to one (S^{2-}). Therefore, the presence of heavy packed ions in the unit cell resulted in more gamma attenuation. The Z_{eff} variation with the energy range of 0.015–15 MeV may be associated with the density, mean atomic number, composition (%) or weight fraction, total atomic cross-section, crystal geometry and elemental packing of each molecule. It can be concluded that Ag_2S was the superior attenuator between the sulphides under prediction, especially at higher energies. The Gamma Protection Efficiency (GPE, %) was also calculated for the gamma shielding subject based on the Linear Attenuation Coefficient (LAC) data presented in the Beer–Lamberts law: GPE% = (1-e^(-μx)) * 100, where the thickness was assumed. The GPE% increased with increasing thickness and decreased with increasing energy. Also, silver sulphide showed the highest GPE among the other tested materials. The GPE% of the thermal or fast neutrons was also calculated, where the increasing order was **SnS, SnS_2, ZnS, MoS_2,** As_2S_3, $CuFeS_2$, FeS, CoS, and Ag_2S for thermal neutrons and SnS_2, SnS, MoS_2, As_2S_3, ZnS, $CuFeS_2$, FeS, Ag_2S, and CoS for fast neutrons.

1. Introduction

Radiation in both ionizing and nonionizing forms is defined as energy that can be transferred through a medium as a wave or particle. X-rays or gamma rays are non-ionizing radiation (neutral radiation or not electrically charged) that can easily penetrate a target. It is important to control gamma ray exposure by designing an effective protector against this electromagnetic radiation [1, 2]. Like other countries in the world, the Gamma attenuation performance in Iraqi studies has been by characterized by experimental and/or theoretical studies,

depending on the Mass Attenuation Coefficient, Effective Atomic Number, and other parameters. Experimental testing is time-consuming and may involve several sources of error, which can be minimized by computer-based models [3-15].

Various computerized models, such as XCOM, NGCAL, Phy-X/PSD, GRASP, and ParShield, have been developed to calculate attenuation parameters. High attenuation or high photoelectric absorption requires a radiation absorber with a high density (ρ) and Effective Atomic Number (Zeff). The thickness of the tested absorber is another important parameter, especially for materials with lower ρ and Zeff values. Each tested computer-based model has its limitations; for example, XCOM does not calculate all Gamma Shielding parameters in the energy range (1 KeV to 100 GeV). Compared to XCOM, Phy-X/PSD is a downloadable software that requires academic email for registration and covers a narrow energy range (0.015 MeV – 15 MeV), but it calculates many elements, compounds, and other identified materials [4, 16].

Al-Saeedi team thermally manufactured a novel Pb-silicate glass from Iraqi sand and 35% PbO, and the resulting gamma shielding properties were characterized experimentally with Cs-137 and Co-60. The experimental data were compared with the Phy-X/PSD program in the same energy range (0.015-15) MeV, where the linear attenuation coefficient decreased with increasing energy [17].

Sameer and Ali studied red clay with/without boron at various thicknesses. The experimental (Cs-137) and theoretical (XCOM) results showed that the presence of boron caused an increase in the Mass Attenuation Coefficient in addition to the influence of the thickness factor [18].

Two Iraqi researchers [19] reported that the Mass Attenuation Coefficient decreased with increasing nanoparticle content in polyvinyl alcohol and nanobarium sulfate blends. The performance of these blends was evaluated with ^{133}Ba, ^{22}Na, ^{137}Cs, and ^{60}Co radioactives.

Recently, Ghafoor and Shawn [20] reported the Half Value Thickness (HVT) of glass and aluminium, which resulted in a greater shielding of 0.662 MeV of gamma radiation emitted from Cs-137 than from concrete, lead, and iron.

Various nano-bismuth trioxide- and nano-trioxide-doped PMMA materials were constructed by Mahmood et al. for Bi-207 and Cs-137 Linear Attenuation Coefficient, Transmittance, and Absorptivity measurements. The results showed that these doped materials were good protecting agents [21].

El-Sawy and Sarwat [22] studied the gamma shielding parameters of four epoxy–concrete samples and compared them with those of the Win X-COM, Mont Carlo Code (MCNP-5), and artificial neural network (ANN) methods. Both the theoretical and experimental results showed good attenuation characteristics.

Here, various sulphides were investigated theoretically by two online models. Phy-X software was used to compute the Mass Attenuation Coefficient (MAC), Half Value Layer (HVL), Mean Free Path (MFP), and Effective Atomic Number (Zeff), while online NGCAL software was used to compute the linear attenuation coefficient (LAC) and Tenth Value Layer (TVL)) in addition to the calculated Phy-X parameters according to the influence of photons (0.1, 1, 15) MeV, fast neutrons (4 MeV), and thermal neutrons (25.5 meV). The choice of these newly tested (Ag_2S, As_2S_3, CoS, $CuFeS_2$, FeS, MoS_2, SnS, SnS_2, ZnS) materials mainly depended on their metallic atomic number, their insolubilities in water, and their impact on the environment.

2. Experimental and Theoretical Part

Nine sulphides (Ag_2S, As_2S_3, CoS, $CuFeS_2$, FeS, MoS_2, SnS, SnS_2, and ZnS) were selected for this work, and their important properties are tabulated in Table (1), which was collected from the Merck Index and trusted websites. The most important factor of the selection step was their insolubility in water for health and environmental reasons. Furthermore, Table (2) shows the density, mean atomic number, and percentage of chemical composition of the tested sulphides that are used in this theoretical prediction.

Table (1): General information of the sulphides under testing.

Chemical structure	General notes
Ag_2S	Naturally, as argentite Grayish-black, monoclinic (β-form), stable below 179 °C, body centered cubic (α-form), and face-centered cubic (γ-form), α-form: cI8, cubic β-form: mP12, monoclinic; Cubic, cF12; γ-form: cf12, cubic α-form: a = 4.23 Å, b = 6.91 Å, c = 7.87 Å, α = 90°, β = 99.583°, γ = 90° mp 845ºC, insol. H_2O, Sol. HNO_3 and alkali cyanides Use: semiconductor Skin and eye irritations. Argyria
As_2S_3	Naturally: Orpiment Dark yellow solid Crystalline (ruffled sheet) and amorphous (highly cross-linked) forms of trigonal pyramidal (As^{3+}) linked by sulphide a = 1147.5(5) pm, b = 957.7(4) pm, c = 425.6(2) pm α = 90°, β = 90.68(8)°, γ = 90° insol. in H_2O Glass forming, semiconductor. IR transmitting glass, pigment, tanning Acute and chronic toxic to aqua environment
CoS	Naturally: Jaipurite Black, octahedral (β-form) a: 3.35 Å, b: 3.35 Å, c: 5.14 Å, α: 90.00 °, β: 90.00 °, γ: 120.00 °, Volume: 49.84 Å³ Insol. in H_2O Semiconductor, Catalyst of hydrodesulfurization Allergy or asthma symptoms, cancer by inhalation, Damage the unborn, Very toxic to aquatic life: acute with long lasting effects
$CuFeS_2$	Yellow brass- or bronze- crystals. a = 5.289 Å, c = 10.423 Å; Z = 4, Tetragonal crystal system. mp 950ºC, Sol. HNO_3 and aqua regia. Insol. HCl
FeS	Colorless gray to brownish-black lumps, rods or granular powder Hexagonal crystals, a: 3.59 Å, b: 3.59 Å, c: 5.27 Å, α: 90.00 °, β: 90.00 °, γ: 90.00 ° Volume: 67.99 Å³ mp 1194ºC Practically insol in H_2O. Sol. acids
MoS_2	Lead-gray powder, hexagonal, Trigonal prismatic (Mo^{IV}), Pyramidal (S^{2-}), a: 3.19 Å, b: 3.19 Å, c: 13.38 Å, α: 90.00 °, β: 90.00 °, γ: 120.00 ° Volume: 118.07 Å³ mp 2375ºC Insol in dil. acid or water LC_{50} (rat) > 2,820 mg/m³/4 h
SnS	herzenbergite (α-SnS) at 905 K, second order phase transition to β-SnS Gray crystals or black amorphous powder a= 11.18 Å, b = 3.98 Å, c = 4.32, α; 90.00 °, β: 90.00 °, γ: 90.00 °, Volume: 204.32 Å³ Insol. in H_2O, alkali hydroxide or sulphide. Sol. in conc. HCl, hot conc. H_2SO_4 Photovoltaic Irritant (eye, skin, respiratory)
SnS_2	Golden leaflets with metallic luster; hexagonal a = 3.65 Å, c = 5.88 Å, α = 90°, β = 90°, γ = 120°, volume: 144.39 Å³ Insol in H_2O or dil. acid. Sol. in aqua regia, alkali hydroxides or sulphides Gilding and bronzing metals, wood, and paper. Irritant
ZnS	White to grayish-white or yellowish powder, cubic, a: 5.39 Å, b: 5.39 Å, c: 5.39 Å, α: 90.00 °, β: 90.00 °, γ: 90.00 °, Volume:156.36 Å³ Insol in H_2O, alkali. Sol in dil. mineral acids. Pigment for paints, leather, den tal rubber, X-ray screens. irritation (respiratory, eye)

Table (2): Density, mean atomic number, and percentage of chemical composition of sulphides.

Chemical structure	Density, g/cm^3	Mean atomic number, $\bar{Z}$	Composition, %
Ag_2S	7.234	36.66	Ag: 87.06 S: 12.94
As_2S_3	3.64	22.8	As: 60.90 S 39.10
CoS	5.4	21.5	Co: 64.76 S 35.24
$CuFeS_2$	4.1	21.75	Cu: 33.6 Fe: 30.43 S: 34.94
FeS	4.84	21	Fe: 63.52 S 36.48
MoS_2	5.06	24.66	Mo: 59.94 S: 40.06
SnS	5.08	33	Sn: 78.73 S 21.27
SnS_2	4.5	27.33	Sn: 64.92 S: 35.08
ZnS	4.087	23	Zn: 67.10 S: 32.90

Phy-X software was used to compute the Mass Attenuation Coefficient (MAC, cm2/g), Half Value Layer (HVL), Mean Free Path (MFP), and Effective Atomic Number (Zeff) (Tables 3-6). In addition, theoretical parameters that can be calculated by the online NGCAL software include the Mass Attenuation Coefficient (MAC, cm^2/g), Linear Attenuation Coefficient (LAC, cm-1), Half Value Layer (HVL), Tenth Value Layer (TVL), and Mean Free Path (MFP), as mentioned in Tables (7 and 8), according to the influence of photons (0.1, 1, 15) MeV, fast neutrons (4 MeV), and thermal neutrons (25.5 meV).

Table (3): Phy-X software results of the Mass Attenuation Coefficient (MAC) of the tested sulphides.

E, MeV	Ag_2S	As_2S_3	CoS	$CuFeS_2$	FeS	MoS_2	SnS	SnS_2	ZnS
1.50E-02	266.298	66.075	248.627	48.429	202.879	23.313	203.294	35.719	243.437
2.00E-02	121.891	30.421	111.810	21.863	90.808	50.365	93.078	16.286	111.013
3.00E-02	232.986	9.994	35.688	7.005	28.869	17.687	167.122	27.499	35.930
4.00E-02	109.209	4.503	15.945	3.133	12.901	8.151	78.761	12.958	16.092
5.00E-02	60.034	2.442	8.691	1.705	7.050	4.454	43.423	7.151	8.718
6.00E-02	36.694	1.500	5.416	1.060	4.420	2.724	26.696	4.405	5.372
8.00E-02	16.935	0.728	2.760	0.536	2.286	1.280	12.393	2.057	2.642
1.00E-01	9.444	0.443	1.782	0.342	1.500	0.738	6.924	1.159	1.635
1.50E-01	3.558	0.219	1.003	0.189	0.870	0.313	2.599	0.448	0.845
2.00E-01	1.994	0.156	0.771	0.144	0.679	0.197	1.445	0.257	0.619
3.00E-01	1.085	0.113	0.596	0.110	0.530	0.126	0.773	0.145	0.460
4.00E-01	0.803	0.095	0.514	0.095	0.460	0.101	0.567	0.109	0.392
5.00E-01	0.669	0.085	0.462	0.085	0.414	0.088	0.470	0.092	0.350
6.00E-01	0.589	0.077	0.424	0.078	0.380	0.080	0.412	0.081	0.320
8.00E-01	0.493	0.067	0.369	0.068	0.331	0.068	0.343	0.068	0.278
1.00E+00	0.433	0.060	0.331	0.061	0.297	0.061	0.301	0.060	0.249
1.50E+00	0.348	0.049	0.270	0.050	0.242	0.049	0.242	0.048	0.202
2.00E+00	0.307	0.043	0.235	0.043	0.211	0.043	0.213	0.042	0.177
3.00E+00	0.271	0.036	0.198	0.036	0.177	0.037	0.188	0.037	0.150

E, MeV	Ag_2S	As_2S_3	CoS	$CuFeS_2$	FeS	MoS_2	SnS	SnS_2	ZnS
4.00E+00	0.258	0.033	0.179	0.033	0.160	0.034	0.178	0.035	0.136
5.00E+00	0.254	0.031	0.169	0.031	0.150	0.033	0.175	0.034	0.129
6.00E+00	0.254	0.030	0.163	0.030	0.145	0.032	0.174	0.033	0.125
8.00E+00	0.260	0.030	0.157	0.029	0.139	0.032	0.178	0.034	0.122
1.00E+01	0.269	0.030	0.156	0.029	0.138	0.032	0.184	0.034	0.122
1.50E+01	0.293	0.031	0.158	0.029	0.140	0.034	0.200	0.037	0.125

Table (4): Phy-X results of the Effective Atomic Number (Zeff) of the tested sulphides.

E, MeV	Ag_2S	As_2S_3	CoS	$CuFeS_2$	FeS	MoS_2	SnS	SnS_2	ZnS
1.50E-02	42.51	30.07	24.95	25.61	23.98	29.31	42.55	37.78	27.91
2.00E-02	42.73	30.23	25.02	25.70	24.04	38.65	42.90	38.25	28.01
3.00E-02	46.24	30.34	25.04	25.74	24.06	38.97	48.59	47.29	28.06
4.00E-02	46.24	30.25	24.96	25.66	23.98	38.93	48.60	47.31	27.98
5.00E-02	46.18	30.01	24.80	25.49	23.82	38.69	48.50	47.13	27.81
6.00E-02	46.08	29.67	24.57	25.25	23.61	38.29	48.32	46.79	27.55
8.00E-02	45.73	28.76	24.03	24.66	23.12	37.12	47.71	45.72	26.90
1.00E-01	45.24	27.74	23.48	24.05	22.64	35.65	46.86	44.25	26.19
1.50E-01	43.65	25.66	22.53	22.97	21.83	31.97	44.13	39.99	24.80
2.00E-01	42.02	24.49	22.08	22.44	21.46	29.38	41.43	36.31	24.05
3.00E-01	39.75	23.53	21.74	22.04	21.19	26.88	37.77	32.01	23.45
4.00E-01	38.58	23.20	21.63	21.91	21.10	25.93	35.93	30.10	23.25
5.00E-01	37.96	23.06	21.58	21.85	21.07	25.48	34.99	29.17	23.16
6.00E-01	37.62	22.99	21.56	21.82	21.05	25.25	34.45	28.66	23.11
8.00E-01	37.26	22.91	21.54	21.79	21.03	25.02	33.90	28.15	23.07
1.00E+00	37.09	22.88	21.53	21.78	21.02	24.92	33.64	27.91	23.05
1.50E+00	36.99	22.87	21.52	21.78	21.02	24.86	33.48	27.76	23.04
2.00E+00	37.14	22.92	21.55	21.81	21.04	24.98	33.68	27.94	23.08
3.00E+00	37.65	23.11	21.63	21.90	21.11	25.37	34.37	28.59	23.22
4.00E+00	38.16	23.32	21.73	22.01	21.19	25.80	35.09	29.27	23.36
5.00E+00	38.62	23.52	21.82	22.11	21.26	26.20	35.74	29.91	23.50
6.00E+00	38.99	23.69	21.90	22.20	21.33	26.55	36.28	30.45	23.63
8.00E+00	39.58	23.99	22.03	22.35	21.44	27.13	37.14	31.34	23.84
1.00E+01	40.01	24.22	22.14	22.47	21.53	27.58	37.78	32.02	24.00
1.50E+01	40.66	24.59	22.32	22.66	21.68	28.32	38.78	33.13	24.27

Table (5): Phy-X results of the Mean Free Path (MFP) of the tested sulphides.

E, MeV	Ag_2S	As_2S_3	CoS	$CuFeS_2$	FeS	MoS_2	SnS	SnS_2	ZnS
1.50E-02	0.004	0.004	0.004	0.005	0.005	0.008	0.005	0.006	0.004
2.00E-02	0.008	0.010	0.009	0.011	0.011	0.004	0.011	0.014	0.009
3.00E-02	0.004	0.029	0.028	0.035	0.035	0.011	0.006	0.008	0.028
4.00E-02	0.009	0.064	0.063	0.078	0.078	0.024	0.013	0.017	0.062
5.00E-02	0.017	0.118	0.115	0.143	0.142	0.044	0.023	0.031	0.115
6.00E-02	0.027	0.193	0.185	0.230	0.226	0.073	0.037	0.050	0.186
8.00E-02	0.059	0.397	0.362	0.455	0.437	0.154	0.081	0.108	0.379
1.00E-01	0.106	0.653	0.561	0.712	0.667	0.268	0.144	0.192	0.611
1.50E-01	0.281	1.322	0.997	1.289	1.150	0.632	0.385	0.496	1.184
2.00E-01	0.502	1.858	1.297	1.695	1.473	1.001	0.692	0.864	1.617
3.00E-01	0.922	2.565	1.679	2.211	1.885	1.564	1.293	1.536	2.175
4.00E-01	1.246	3.038	1.944	2.568	2.176	1.947	1.764	2.040	2.554
5.00E-01	1.494	3.415	2.164	2.861	2.417	2.240	2.129	2.424	2.859
6.00E-01	1.697	3.741	2.359	3.121	2.632	2.485	2.427	2.740	3.125
8.00E-01	2.030	4.315	2.707	3.583	3.018	2.902	2.914	3.261	3.597
1.00E+00	2.312	4.830	3.022	4.002	3.369	3.266	3.324	3.703	4.022
1.50E+00	2.874	5.936	3.710	4.914	4.135	4.029	4.139	4.598	4.941
2.00E+00	3.255	6.799	4.260	5.639	4.750	4.599	4.694	5.232	5.662
3.00E+00	3.688	8.011	5.058	6.689	5.652	5.354	5.331	6.012	6.684
4.00E+00	3.877	8.771	5.583	7.374	6.252	5.787	5.618	6.410	7.330
5.00E+00	3.941	9.240	5.928	7.821	6.652	6.029	5.724	6.597	7.736
6.00E+00	3.942	9.520	6.149	8.103	6.911	6.152	5.736	6.666	7.982
8.00E+00	3.852	9.748	6.366	8.376	7.177	6.202	5.621	6.617	8.189
1.00E+01	3.721	9.746	6.422	8.438	7.258	6.128	5.442	6.465	8.204
1.50E+01	3.414	9.452	6.318	8.283	7.168	5.826	5.005	6.031	7.981

Table (6): Phy-X results of the half value layer (HVL) of the tested sulphides.

E, MeV	Ag_2S	As_2S_3	CoS	$CuFeS_2$	FeS	MoS_2	SnS	SnS_2	ZnS
1.50E-02	0.003	0.003	0.003	0.003	0.003	0.006	0.003	0.004	0.003
2.00E-02	0.006	0.007	0.006	0.008	0.008	0.003	0.007	0.009	0.006
3.00E-02	0.003	0.020	0.019	0.024	0.024	0.008	0.004	0.006	0.019
4.00E-02	0.006	0.044	0.043	0.054	0.054	0.017	0.009	0.012	0.043
5.00E-02	0.012	0.082	0.080	0.099	0.098	0.031	0.016	0.022	0.080
6.00E-02	0.019	0.134	0.128	0.160	0.157	0.050	0.026	0.035	0.129
8.00E-02	0.041	0.275	0.251	0.316	0.303	0.107	0.056	0.075	0.262
1.00E-01	0.073	0.453	0.389	0.494	0.462	0.186	0.100	0.133	0.424
1.50E-01	0.195	0.916	0.691	0.894	0.797	0.438	0.267	0.344	0.821
2.00E-01	0.348	1.288	0.899	1.175	1.021	0.694	0.480	0.599	1.121
3.00E-01	0.639	1.778	1.164	1.532	1.307	1.084	0.896	1.065	1.508

E, MeV	Ag_2S	As_2S_3	CoS	$CuFeS_2$	FeS	MoS_2	SnS	SnS_2	ZnS
4.00E-01	0.863	2.106	1.348	1.780	1.508	1.350	1.223	1.414	1.770
5.00E-01	1.036	2.367	1.500	1.983	1.675	1.553	1.475	1.680	1.981
6.00E-01	1.176	2.593	1.635	2.163	1.825	1.723	1.682	1.899	2.166
8.00E-01	1.407	2.991	1.876	2.484	2.092	2.011	2.020	2.260	2.493
1.00E+00	1.602	3.348	2.095	2.774	2.335	2.264	2.304	2.567	2.788
1.50E+00	1.992	4.114	2.572	3.406	2.866	2.792	2.869	3.187	3.425
2.00E+00	2.256	4.713	2.953	3.909	3.292	3.188	3.253	3.627	3.924
3.00E+00	2.556	5.553	3.506	4.637	3.918	3.711	3.695	4.167	4.633
4.00E+00	2.687	6.080	3.870	5.112	4.333	4.012	3.894	4.443	5.081
5.00E+00	2.732	6.405	4.109	5.421	4.611	4.179	3.967	4.573	5.362
6.00E+00	2.733	6.599	4.262	5.617	4.791	4.264	3.976	4.620	5.532
8.00E+00	2.670	6.757	4.412	5.806	4.975	4.299	3.896	4.587	5.676
1.00E+01	2.579	6.756	4.452	5.849	5.031	4.247	3.772	4.481	5.687
1.50E+01	2.367	6.551	4.379	5.741	4.969	4.038	3.469	4.181	5.532

Table (7): Mass and linear attenuation factors of the tested sulphides by NGCAL software.

Sample ID	Mass Attenuation factor. cm^2/g					Linear Attenuation factor. cm^{-1}				
	Neutrons		Photons			Neutrons		Photons		
	Thermal (25.4 meV)	Fast (4MeV)	0.1 MeV	1 MeV	15 MeV	Thermal (25.4 meV)	Fast (4MeV)	0.1 MeV	1 MeV	15 MeV
Ag_2S	0.3118	0.0029	1.3059	0.0598	0.0405	2.2555	0.02069	9.4470	0.4326	0.2929
As_2S_3	0.0263	0.0004	0.4426	0.0599	0.0306	0.0909	0.0012	1.5315	0.2071	0.1058
CoS	0.2813	0.0318	0.3269	0.0607	0.0290	1.5335	0.1735	1.7818	0.3309	0.1583
$CuFeS_2$	0.0275	0.0032	0.3424	0.0610	0.02945	0.1125	0.01297	1.4039	0.2499	0.1207
FeS	0.0240	0.0028	0.3098	0.0613	0.0288	0.1159	0.01349	1.4994	0.2968	0.1395
MoS_2	0.0135	0.0002	0.7378	0.0605	0.0339	0.0684	0.0010	3.7334	0.3062	0.1717
SnS	0.0047	0.0001	1.3625	0.0592	0.0393	0.0240	0.0006	6.9216	0.3008	0.1998
SnS_2	0.0057	0.0001	1.1590	0.0600	0.0368	0.0255	0.0005	5.2155	0.2700	0.1658
ZnS	0.0107	0.0005	0.4001	0.0608	0.0307	0.0435	0.0021	1.6354	0.2486	0.1253

Table (8): MFP, HVL, and TVL data of the tested sulphides obtained by the NGCAL software.

Sample ID	Mean Free Path (for Photons). cm			Half Value Layer (for Photons). cm			Tenth-value layer (for Photons). cm		
	0.1 MeV	1 MeV	15 MeV	0.1 MeV	1 MeV	15 MeV	0.1 MeV	1 MeV	15 MeV
Ag_2S	0.1059	2.3118	3.4146	0.0734	1.6024	2.3668	0.2437	5.3232	7.8624
As_2S_3	0.6530	4.8295	9.4518	0.4526	3.3475	6.5515	1.5035	11.1203	21.7635
CoS	0.5613	3.0226	6.3178	0.3890	2.0951	4.3792	1.2923	6.9597	14.5473
$CuFeS_2$	0.71230	4.0020	8.283	0.4937	2.7740	5.7411	1.6401	9.2149	19.0715
FeS	0.6669	3.3689	7.16836	0.4623	2.3352	4.9687	1.5356	7.7572	16.5058
MoS_2	0.2679	3.2656	5.8252	0.1857	2.2636	4.0377	0.6168	7.5194	13.4130
SnS	0.1445	3.3241	5.0056	0.1001	2.3041	3.4696	0.3327	7.6541	11.5258
SnS_2	0.19174	3.7031	6.0315	0.1329	2.5668	4.1807	0.4415	8.5267	13.8881
ZnS	0.6115	4.0222	7.9808	0.4239	2.7880	5.5318	1.4080	9.2615	18.3764

4. Results and Discussion

The calculated gamma and neutron parameters in the studied energy range were found via Phy-X and NGCAL software (Tables 3-8). Table (9) displays the linear attenuation coefficients and the differences (Δ%) between both models (Equation 1) [23, 24]:

$$\Delta\% = (\mu_{Phy\text{-}X} - \mu_{NGCAL})/\mu_{Phys\text{-}X})* 100 \ldots\ldots (1)$$

Table (9): Percentages of differences (Δ%) between the Phy-X and NGCAL results depending on LAC.

Sulphide	Energy MeV	LAC in Phy-X	LAC in NGCAL	Δ%
Ag_2S	0.1	9.444	9.4470	-0.031766201
	1	0.433	0.4326	0.092378753
	15	0.293	0.2929	0.034129693
As_2S_3	0.1	1.531	1.5315	-0.032658393
	1	0.207	0.2071	-0.048309179
	15	0.106	0.1058	0.188679245
CoS	0.1	1.782	1.7818	0.011223345
	1	0.331	0.3309	0.03021148
	15	0.158	0.1583	-0.189873418
$CuFeS_2$	0.1	1.404	1.4039	0.007122507
	1	0.250	0.2499	0.04
	15	0.121	0.1207	0.247933884
FeS	0.1	1.500	1.4994	0.04
	1	0.297	0.2968	0.067340067

Sulphide	Energy MeV	LAC in Phy-X	LAC in NGCAL	Δ%
	15	0.140	0.1395	0.357142857
MoS_2	0.1	0.738	3.7334	-405.8807588
	1	0.061	0.3062	-401.9672131
	15	0.034	0.1717	-405
SnS	0.1	6.924	6.9216	0.034662045
	1	0.301	0.3008	0.066445183
	15	0.200	0.1998	0.1
SnS_2	0.1	5.218	5.2155	0.047911077
	1	0.270	0.2700	0
	15	0.166	0.1658	0.120481928
ZnS	0.1	1.635	1.6354	-0.024464832
	1	0.249	0.2486	0.16064257
	15	0.125	0.1253	-0.24

Table (9) confirms that the Phy-X results were in good agreement with the NGCAL results, where Δ% was less than 1%.

The Mass Attenuation Coefficient (MAC) was calculated by both software programs, and the resulting MAC values decreased with increasing incident energy depending on photon or neutron interactions with the material. Photoelectric absorption usually occurs in the low-energy region, and the probability of this energic event (cross-section) changes with the atomic number and the applied energy [23-26].

Commonly, neutrons are categorized as fast or thermal, where fast neutrons can be generated by fission chains in a nuclear reactor containing enriched uranium. Neutron collision with the target atomic nucleus leads to scattering, capture, and fission, and these noncharge particles indirectly ionize the tested material after penetration [26, 27].

From Table (7) and Figure (1), several remarkable notes were noted, such as the following:

- For thermal neutrons (25.4 MeV), the MAC sequence was SnS (lowest value), SnS_2, ZnS, MoS_2, FeS, As_2S_3, $CuFeS_2$, CoS, and Ag_2S (highest value).
- Fast neutrons were poorly shielded by SnS or SnS_2, while cobalt sulphide was a superior neutron attenuator.
- The numeric MAC order with fast neutrons (4 MeV) was SnS, SnS_2, MoS_2, As_2S_3, ZnS, FeS, Ag_2S, $CuFeS_2$, and CoS (Table 7).
- MAC - Photon attenuation by NGCAL varied according to the applied energy, where the highest value belonged to SnS and the lowest was observed for FeS at 0.1 MeV.
- MAC values at 1 MeV and 1 MeV gave nonidentical sequences, where FeS and Ag_2S had the highest MAC values at 1 MeV and 15 MeV, respectively.
- Moreover, LAC values in NGCAL showed another increasing sequence in comparison to those in MAC, which was mainly affected by the density of each compound.
- The LAC values showed that Ag_2S had the highest value at all incident energies. In conclusion, the MAC and LAC determined by the NGCAL model indicated that Ag_2S is a superior photon attenuator, especially at 15 MeV.

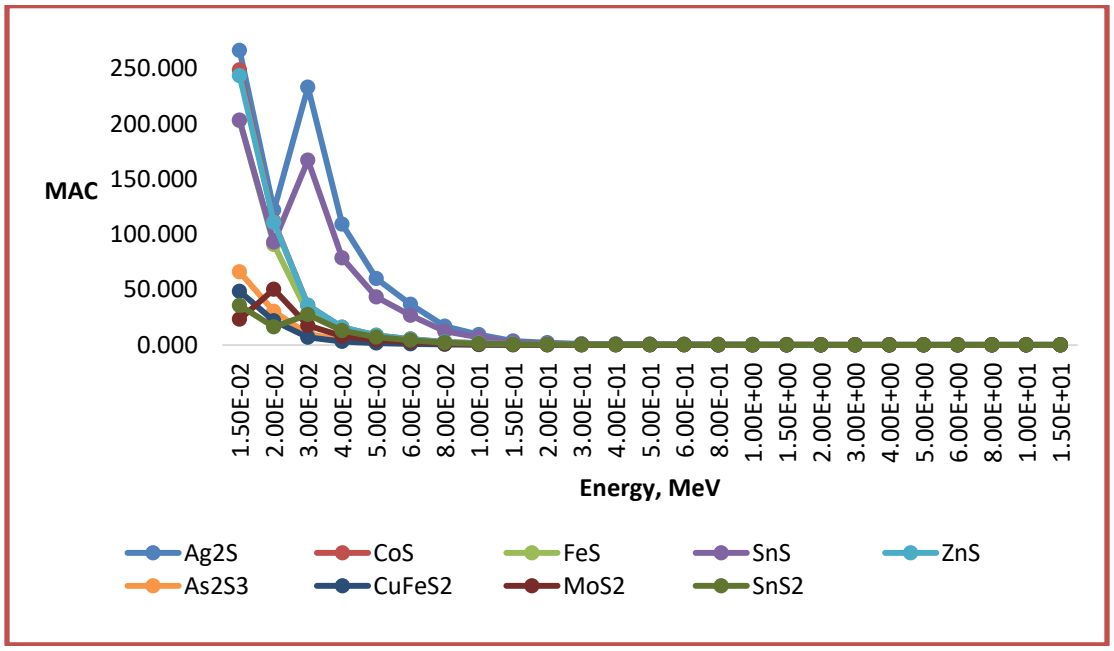

Figure (1): Mass Attenuation Coefficient for sulphides calculated by Phy-X.

According to the Phy-X model, the following general observations can be made:

- The highest MAC value was found for Ag_2S in all tested energy ranges.
- $CuFeS_2$ showed the lowest MAC value, ranging from 0.03 MeV to 15 MeV.
- Here, Ag_2S contains two silver (Ag^+) ions with the highest density (7.234 gm/cm^3), mean atomic number $\bar{Z}$ (36.66), and metal composition (Ag%: 87.06), and has the lowest density (S%= 12.94) among the sulphides under evaluation.
- $CuFeS_2$ contains nonidentical ions (Cu^{2+} and Fe^{2+}), where Cu%: 33.6 and Fe%: 30.43, and the metal composition for both ions is 64.03, which is less than that of Ag%= 87.06.
- Furthermore, the content of sulphide, a nonmetallic ion contained in both compounds, was greater in $CuFeS_2$ (34.94%) than in Ag_2S (12.94%) (Tables 1 and 2).
- Also, in Ag_2S, a monoclinic structure is present at room temperature where this β-form has space group P21/c, a = 4.229 Å, b = 6.931 Å, c = 7.862 Å; β = 99.61°; and Z=4 and its network is fabricated from two silver ions ($2Ag^+$) linked to one sulphide ion (S^{2-}).
- CuFeS2 in its tetrahedral structure, where (2Cu2+ and 2Fe2+) are coordinated to (4S2-), which is a space group (I42d), and the unit cell edge lengths are a = 5.289 Å, c = 10.423 Å, and Z = 4.
- From these crystal lattice data, it can be concluded that the presence of heavy packed ions in the unit cell resulted in more gamma attenuation (Table 1).

By Phy-X estimation, the following monosaccharides (FeS, CoS, ZnS, SnS, and Ag_2S) were identified:

- The MAC increases with increasing mean atomic number and metal content.
- The same result was observed for disulphides ($CuFeS_2$, MoS_2, and SnS_2).
- It can be concluded that more metal ion packing or volume may lead to an increase in gamma attenuation.
- In this study, Mean Free Path (MFP) values, which are the average distance between two successive interactions made by photons, were also calculated by both mathematical models (Tables 5 and 8, Figure 2):
- A good agreement in the lowest and highest MFPs was detected at 0.1 MeV and 1 MeV for Ag_2S, $CuFeS_2$ and Ag_2S and As_2S_3, respectively.
- At 15 MeV, the NGCAL calculations included Ag_2S and FeS, while Phy-X included Ag_2S and As_2S_3.

- Ag_2S had the greatest effect on all tested incident energies, as this medium quickly interacted with the photon source compared to the other tested sulphides.

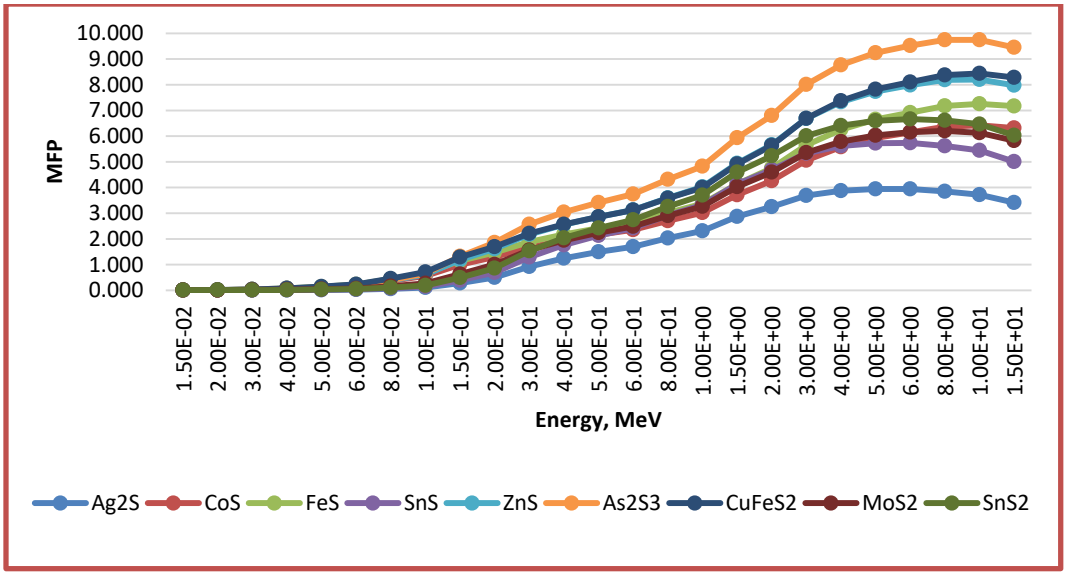

Figure (2): Mean Free Path (MFP) of the tested sulphides.

The Half Value Layer (HVL), as another shielding character, describes the thickness of the tested material where 50% of the initial radiation intensity passes through the material. To describe radiation attenuation, the lower Half Value Layer signifies the shielding capability of the tested material, where HVL is calculated according to ($\text{HVL} = \frac{0.693}{\mu}$), where μ is the linear attenuation coefficient. In general, a lower HVL indicates excellent gamma shielding. The HVL at lower energies (less than 0.1 MeV) depends on the chemical composition, particularly the mean atomic number, while the influence of energy becomes more pronounced at > 0.1 MeV due to the photoelectric mechanism [23-28].

As shown in Table (2), As_2S_3 has the lowest density, while Ag_2S has the highest density when the density increases (As_2S_3, ZnS, $CuFeS_2$, SnS_2, FeS, MoS_2, SnS, CoS, and Ag_2S). The presence of sulphides in the chemical composition (%) showed that Ag_2S, which had the lowest S%, followed by $SnS, ZnS, CuFeS_2$, SnS_2, and CoS, FeS, As_2S_3, MoS_2, which had the highest S%. Also, the presence of cations in these sulphides has a major influence on the elemental % arrangement: $CuFeS_2$, MoS_2, As_2S_3, FeS, CoS, SnS_2, ZnS, SnS, and Ag_2S.

In Table (6), the HVL values of each compound tested by the Phy-X model exhibited the following comments:

- The HVL increased with increasing incident energy, followed by irregular HVL data at high energies (8-15) MeV.
- Silver sulphide had the lowest HVL, and arsenic sulphide had the highest value starting at 0.15 MeV.
- The HVL sequence of the tested sulphides at 0.1 MeV was Ag_2S, SnS, SnS_2, MoS_2, CoS, ZnS, As_2S_3, FeS, and $CuFeS_2$
- At 1 MeV, Ag_2S, CoS, MoS_2, SnS, FeS, SnS_2, $CuFeS_2$, ZnS, and As_2S_3.
- At the highest incident energy (15 MeV), the increasing HVL sequence was Ag_2S, SnS, MoS_2, SnS_2, CoS, FeS, ZnS, $CuFeS_2$, and As_2S_3.

According to Table (8), the HVL values at 0.1, 1, and 15 MeV, which were calculated via the NGCAL model, exhibited various increasing trends with respect to the incident energy:

- At 0.1 MeV, the HVL data sequences of Ag_2S, SnS, SnS_2, MoS_2, CoS, ZnS, As_2S_3, FeS, and $CuFeS_2$

- At 1 MeV, Ag_2S, CoS, MoS_2, SnS, FeS, SnS_2, $CuFeS_2$, ZnS, and As_2S_3 were obtained.
- At the highest incident energy (15 MeV), the increasing HVL sequence was Ag_2S, SnS, MoS_2, SnS_2, CoS, FeS, ZnS, $CuFeS_2$, and As_2S_3.
- The HVL sequence at 0.1, 1, and 15 MeV according to both models presented 100% similarity.
- NGCAL and Phy-X showed that silver sulphide was the best material for gamma shielding.

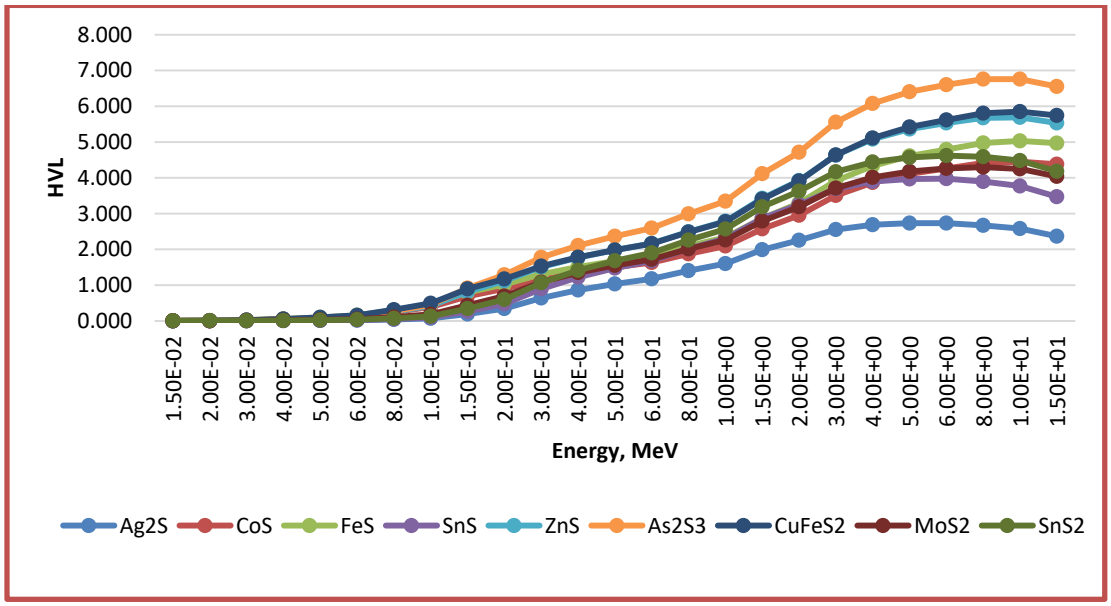

Figure (3): Half Value Layer (HVL) of the tested sulphides.

The Tenth Value Layer (TVL) of all the tested materials were calculated by NGCAL, as shown in Table (8). At 0.1 MeV, the TVL increased in the order of Ag_2S, SnS, SnS_2, MoS_2, CoS, ZnS, As_2S_3, FeS, and $CuFeS_2$. The increasing sequence of TVL was identical to that of HVL at 1 MeV and 15 MeV. The reason behind this similarity is related to the base of calculation, where HVL and TVL mainly depend on LAC data.

The variation in Z_{eff} with the energy range of 0.015–15 MeV was also estimated by the Phy-X model, as shown in Figure (2) and Table (4), depending on the following equations (Eqs. 2–6):

$$\sigma_t = \frac{\mu_m M}{N_A} \quad \text{..... (2)}$$

Where: the total atomic cross-section (σ_t), is the molecular weight of sulphide $M = \sum_i^n n_i A_i$ and N_A is Avogadro's number.

$$\sigma_a = \frac{1}{N_A} \sum f_i A_i \left(\frac{\mu}{\rho}\right)_i \quad \text{..... (3)}$$

Where: (σ_a) is the effective cross-section,

$$\sigma_e = \frac{1}{N_A} \sum \frac{f_i A_i}{Z_i} \left(\frac{\mu}{\rho}\right)_i \quad \text{..... (4)}$$

$$\sigma_e = \frac{\sigma_a}{Z_{eff}} \quad \text{..... (5)}$$

Where the total electronic cross-section (σ_e), where f_i=n/(∑_in_i) signifies the fractional abundance of the elements (i), the number of atoms is ∑_i^n⟦f_i=1⟧, and Z_i is the atomic number of the element. (σ_t) and σ_e are related to the Effective Atomic Number (Z_eff) of the tested material:

$$\mathbf{Z_{eff}} = \frac{\sigma_a}{\sigma_e} \quad \ldots\ldots \mathbf{(6)}$$

This variation was generally ruled by the following sulphide–photon interactions: absorption, scattering, and pair production. The obtained results (Table 4, Figure 4) showed the following:

- Iron sulphide (FeS) had the lowest Z_{eff} values.
- The maximum values of Z_{eff} varied between those of SnS (0.015 MeV to 0.15 MeV) and Ag_2S (0.2-15) MeV.
- The Z_{eff} increasing sequence at 0.015 MeV was FeS, CoS, $CuFeS_2$, ZnS, MoS_2, As_2S_3, SnS_2, Ag_2S, and SnS
- At 0.2 MeV, FeS, CoS, $CuFeS_2$, ZnS, As_2S_3, MoS_2, SnS_2, SnS, and Ag_2S were present.
- The variation in Z_{eff} with respect to energy may be related to the density, mean atomic number, composition (%) or weight fraction, and total atomic cross-section in addition to the crystal geometry and elemental packing of each molecule.

From the obtained Zeff data, it can be concluded that Ag2S was the superior attenuator between the sulphides under prediction, especially at higher energies (Table 4, Figure 4).

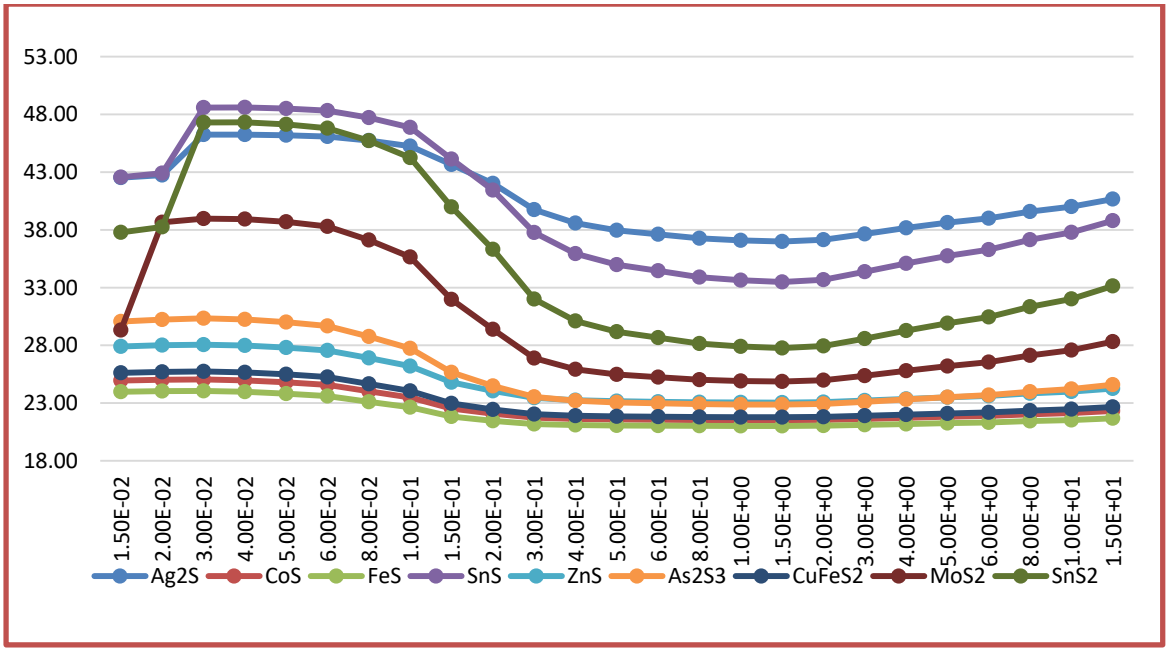

Figure (4): Effective Atomic Number $\boldsymbol{Z_{eff}}$ of the tested sulphides.

The gamma protection efficiency (GPE, %) was also calculated and tabulated. This calculated character in the gamma shielding subject depends on the linear attenuation coefficient (LAC) data presented in the Beer–Lamberts law (Eq. 7 or Eq. 8). Here, I, the intensity of the radiation emitted, and Io, which passed through the tested material, can be measured directly in the laboratory according to the experimental conditions.

$$\boldsymbol{I = I_\circ e^{-\mu x}} \quad \ldots\ldots \mathbf{(7)}$$

$$\boldsymbol{I/I_\circ = e^{-\mu x}} \quad \ldots\ldots \mathbf{(8)}$$

In theoretical calculations, the thickness (x, cm), I, and $I_\circ$ are numerically unavailable; therefore, the Gamma Protection Efficiency (GPE%) thickness is assumed. The calculation of this important characteristic provides more readable images of the ability of a material to attenuate gamma radiation. Additionally, Equation 11 can be used to estimate the GPE% at any energy and thickness of any source by using the linear attenuation coefficient (μ) from any theoretical computing model.

$$\boldsymbol{Efficiency}\ (\boldsymbol{E}\%) = (\boldsymbol{X}_\circ - \boldsymbol{X}/\boldsymbol{X}_\circ) * \mathbf{100}\ \ldots\ldots\ (9)$$

$$\boldsymbol{Gamma\ Protection\ Efficiency}\ (\boldsymbol{GPE}\%) = (\mathbf{1} - \left(\frac{\boldsymbol{I}}{\boldsymbol{I}_\circ}\right)) * \mathbf{100}\ \ldots\ldots\ (10)$$

$$\boldsymbol{Gamma\ Protection\ Efficiency}\ (\boldsymbol{GPE}\%) = (\mathbf{1} - (\boldsymbol{e}^{-\mu x}) * \mathbf{100}\quad \ldots\ldots\ (11)$$

In this study, GPE% was not calculated at 0.015 MeV because GPE% reached the optimum efficiency (100%), as shown in Table 10, with silver sulphide as an example. From Tables (11-23) and Figure (5), the GPE% for gamma shielding increased with increasing thickness and decreased with increasing energy. Additionally, silver sulphide showed the highest GPE% among the other tested materials.

The GPE% of the thermal or fast neutrons were also calculated, where the increasing order was SnS, SnS_2, ZnS, MoS_2, As_2S_3, $CuFeS_2$, FeS, CoS, and Ag_2S for thermal neutrons and SnS_2, SnS, MoS_2, As_2S_3, ZnS, $CuFeS_2$, FeS, Ag_2S, and CoS for fast neutrons (Figures 6 and 7) (Tables 20-23). It can be concluded that silver sulphide can be considered a superior shielding material for neutrons, especially at high energy.

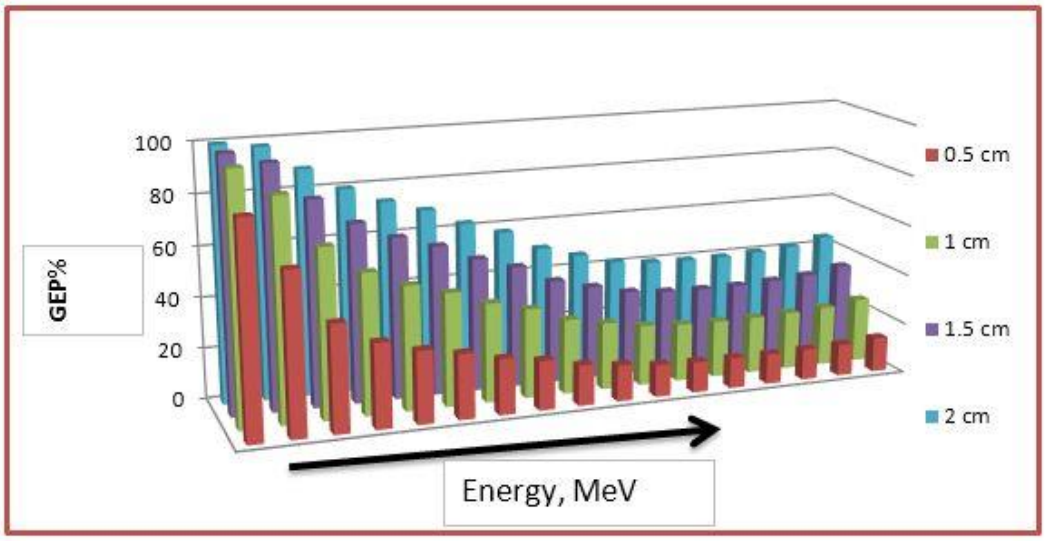

Figure (5): GPE% of silver sulphide with increasing gamma energy at x= 0.5, 1, 1.5, and 2 cm.

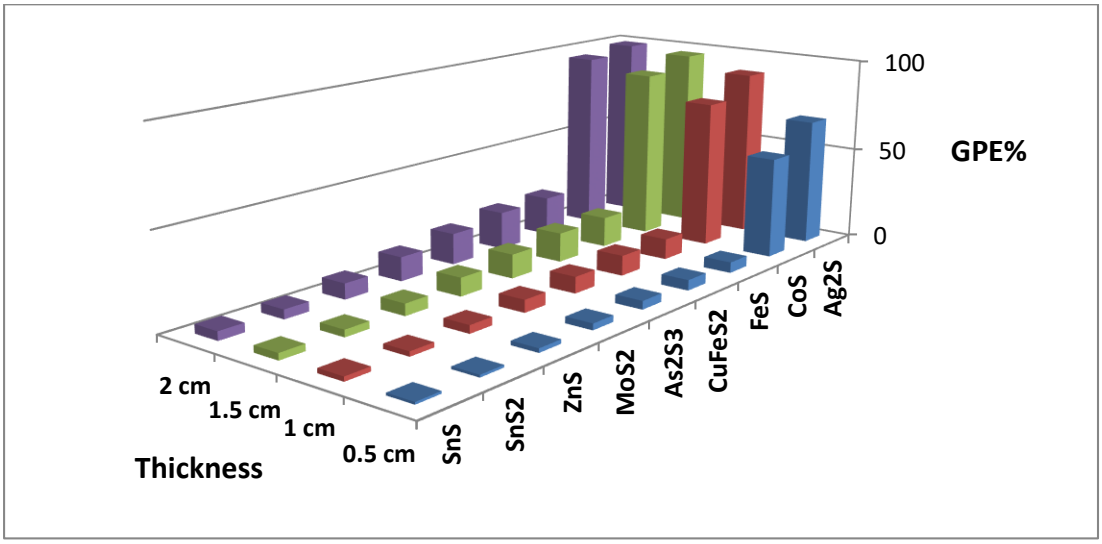

Figure (6): GPE% results of the tested sulphides with thermal neutrons at (x= 0.5, 1, 1.5, 2) cm.

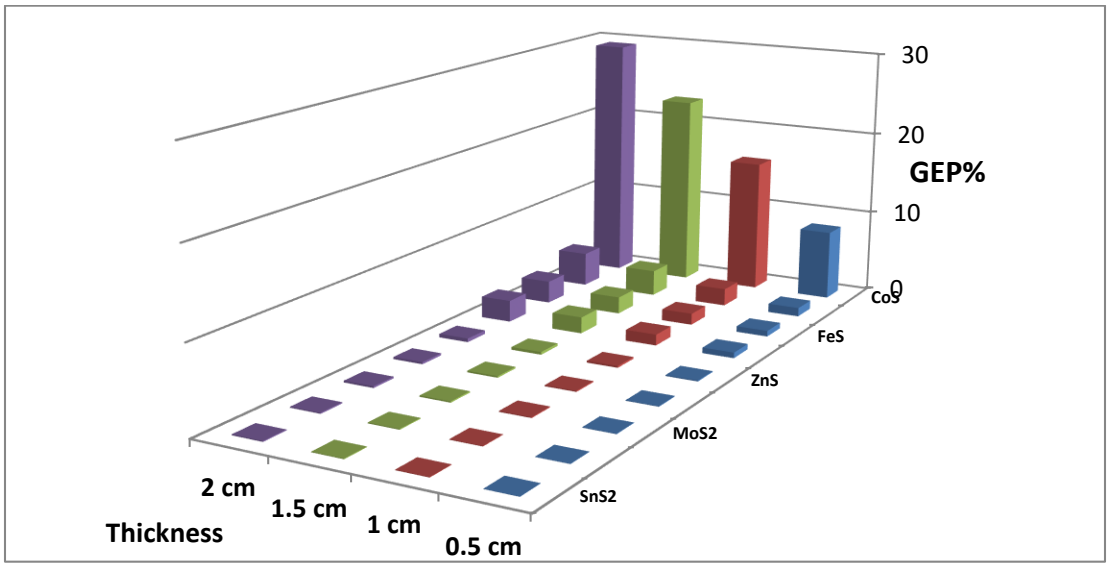

Figure (7): GPE% results of the tested sulphides with fast neutrons at (x= 0.5, 1, 1.5, 2) cm.

Table (10): GPE% of silver sulphide at low energy with 100% value.

1.50E-02	**266.298**	**100**	**100**	**100**	**100**
2.00E-02	121.891	100	100	100	100
3.00E-02	232.986	100	100	100	100
4.00E-02	109.209	100	100	100	100
5.00E-02	60.034	100	100	100	100
6.00E-02	36.694	100	100	100	100
8.00E-02	16.935	99.97898	100	100	100

Table (11): Gamma Protection Efficiency (GPE, %) of Silver Sulphide with different thickness from Phy-X / Linear Attenuation Coefficients.

E, MeV	LAC, cm^{-1}	**Thickness, cm**			
		0.5	**1**	**1.5**	**2**
1.50E-01	**3.558**	**83.12292**	97.15164	99.51928	99.91887
2.00E-01	1.994	63.095	86.38021	94.97362	98.14501
3.00E-01	1.085	41.86381	66.20183	80.35103	88.57684
4.00E-01	0.803	33.06025	55.1907	70.00477	79.92127
5.00E-01	0.669	28.4384	48.78937	63.35285	73.77471
6.00E-01	0.589	25.52112	44.52897	58.6858	69.22965
8.00E-01	0.493	21.83114	38.8963	52.23594	62.66338
1.00E+00	0.433	19.44835	35.11431	47.73351	57.89848
1.50E+00	0.348	15.97036	29.3902	40.66684	50.14256
2.00E+00	0.307	14.23835	26.44939	36.92178	45.90307
3.00E+00	0.271	12.67957	23.75143	33.41942	41.86155
4.00E+00	0.258	12.09908	22.73428	32.08271	40.30008

E, MeV	LAC, cm^{-1}	Thickness, cm			
		0.5	1	1.5	2
5.00E+00	0.254	11.91453	22.4095	31.65404	39.79714
6.00E+00	0.254	**11.91153**	22.40422	31.64706	39.78894
8.00E+00	0.260	12.17181	22.86209	32.25117	40.49743
1.00E+01	0.269	12.57408	23.56709	33.17782	41.5801
1.50E+01	0.293	13.62228	25.3889	35.55264	44.33184

Table (12): Gamma Protection Efficiency (GPE, %) of Arsenic Sulphide with different thickness from Phy-X / Linear Attenuation Coefficients.

E, MeV	LAC	Thickness, cm			
		0.5	1	1.5	2
6.00E-02	5.191	**98.53771**	99.44341	99.95848	99.9969
8.00E-02	2.520	92.53949	91.9531	97.71733	99.35247
1.00E-01	1.531	71.63293	78.37788	89.94581	95.32484
1.50E-01	0.756	53.50041	53.06585	67.84612	77.97186
2.00E-01	0.538	31.4915	41.62199	55.39599	65.92008
3.00E-01	0.390	23.5945	32.28624	44.27945	54.14846
4.00E-01	0.329	17.71163	28.04421	38.96224	48.22365
5.00E-01	0.293	15.17324	25.38504	35.54763	44.32607
6.00E-01	0.267	13.62005	23.45443	33.03003	41.40775
8.00E-01	0.232	12.50967	20.68381	29.36129	37.08943
1.00E+00	0.207	10.94037	18.70292	26.69857	33.90784
1.50E+00	0.168	9.835105	15.50475	22.33087	28.60553
2.00E+00	0.147	8.078704	13.6779	19.7984	25.48494
3.00E+00	0.125	7.09031	11.73466	17.07503	22.0923
4.00E+00	0.114	6.050364	10.77513	15.71916	20.38923
5.00E+00	0.108	5.541086	10.25769	14.98494	19.46318
6.00E+00	0.105	5.267583	9.971098	14.57737	18.94797
8.00E+00	0.103	5.116439	9.750001	14.2625	18.54938
1.00E+01	0.103	**5.000001**	9.751431	14.26454	18.55196
1.50E+01	0.106	5.000753	10.03953	14.67475	19.07114

Table (13): Gamma Protection Efficiency (GPE, %) of Cobalt Sulphide with different thickness from Phy-X / Linear Attenuation Coefficients.

E, MeV	LAC, cm-1	Thickness, cm			
		0.5	1	1.5	2
6.00E-02	5.416	**93.33346**	99.55557	99.97037	99.99802
8.00E-02	2.760	74.84653	93.67303	98.40855	99.59969
1.00E-01	1.782	58.97466	83.16921	93.09511	97.16725
1.50E-01	1.003	39.4442	63.32995	77.79415	86.55307
2.00E-01	0.771	31.98661	53.74179	68.53823	78.60178

E, MeV	LAC, cm-1	Thickness, cm			
		0.5	1	1.5	2
3.00E-01	0.596	25.75892	44.88261	59.08026	69.62074
4.00E-01	0.514	22.67373	40.20649	53.76391	64.24736
5.00E-01	0.462	20.63131	37.00611	50.00257	60.3177
6.00E-01	0.424	19.1028	34.55643	47.05798	57.17139
8.00E-01	0.369	16.86527	30.88617	42.54241	52.23279
1.00E+00	0.331	15.24695	28.1692	39.12121	48.40337
1.50E+00	0.270	12.60693	23.62452	33.25313	41.66786
2.00E+00	0.235	11.07554	20.92441	29.68246	37.47051
3.00E+00	0.198	9.413061	17.94007	25.66442	32.66167
4.00E+00	0.179	8.566313	16.39881	23.56035	30.10841
5.00E+00	0.169	8.0883	15.52239	22.3552	28.63534
6.00E+00	0.163	7.809747	15.00957	21.64711	27.76627
8.00E+00	0.157	7.554018	14.5374	20.99326	26.96145
1.00E+01	0.156	**7.489861**	14.41874	20.82866	26.75848
1.50E+01	0.158	7.608605	14.6383	21.13313	27.1338

Table (14): Gamma Protection Efficiency (GPE, %) of Cupric Ferrous Sulphide with different thickness from Phy-X / Linear Attenuation Coefficients.

E, MeV	LAC, cm-1	Thickness, cm			
		0.5	1	1.5	2
5.00E-02	6.989	**96.96391**	99.90782	99.9972	99.99992
6.00E-02	4.345	88.60946	98.70256	99.85221	99.98317
8.00E-02	2.196	66.64903	88.87713	96.29041	98.76282
1.00E-01	1.404	50.44348	75.44152	87.82967	93.96881
1.50E-01	0.776	32.14496	53.95693	68.75746	78.80036
2.00E-01	0.590	25.54966	44.57147	58.73327	69.27678
3.00E-01	0.452	20.24106	36.38511	49.26144	59.53146
4.00E-01	0.389	17.69124	32.25268	44.23802	54.10301
5.00E-01	0.350	16.034	29.49711	40.80155	50.29343
6.00E-01	0.320	14.80471	27.41763	38.16324	47.31799
8.00E-01	0.279	13.02326	24.35047	34.20251	42.77149
1.00E+00	0.250	11.74444	22.10957	31.25737	39.33081
1.50E+00	0.204	9.675056	18.41405	26.30753	33.43732
2.00E+00	0.177	8.485152	16.25033	23.35661	29.85992
3.00E+00	0.149	7.202247	13.88577	20.08793	25.84339
4.00E+00	0.136	6.555446	12.68115	18.40529	23.75419
5.00E+00	0.128	6.192743	12.00199	17.45148	22.56349
6.00E+00	0.123	5.983867	11.60967	16.89883	21.87149
8.00E+00	0.119	5.794961	11.25411	16.3969	21.24166
1.00E+01	0.119	5.753279	11.17556	16.28587	21.10218

E, MeV	LAC, cm-1	Thickness, cm			
		0.5	1	1.5	2
1.50E+01	0.121	5.858052	11.37294	16.56476	21.45244

Table (15): Gamma Protection Efficiency (GPE, %) of Ferrous Sulphide with different thickness from Phy-X / Linear Attenuation Coefficients.

E, MeV	LAC, cm-1	Thickness, cm			
		0.5	1	1.5	2
5.00E-02	7.050	**97.05529**	99.91329	99.99745	99.99992
6.00E-02	4.420	89.03028	98.79665	99.868	99.98552
8.00E-02	2.286	68.12116	89.8374	96.76028	98.96721
1.00E-01	1.500	52.75325	77.67744	89.45332	95.01704
1.50E-01	0.870	35.26858	58.09844	72.87652	82.44259
2.00E-01	0.679	28.78161	49.27942	63.87762	74.27422
3.00E-01	0.530	23.29631	41.16543	54.87171	65.38494
4.00E-01	0.460	20.5327	36.84949	49.81599	60.12013
5.00E-01	0.414	18.68766	33.88303	46.23875	56.28547
6.00E-01	0.380	17.29975	31.60668	43.43855	53.22354
8.00E-01	0.331	15.26547	28.2006	39.16111	48.44846
1.00E+00	0.297	13.79225	25.68224	35.93233	44.76871
1.50E+00	0.242	11.38848	21.47998	30.42222	38.34607
2.00E+00	0.211	9.991262	18.98427	27.07877	34.36452
3.00E+00	0.177	8.466193	16.21562	23.30897	29.80178
4.00E+00	0.160	7.686576	14.78232	21.33264	27.37946
5.00E+00	0.150	7.241338	13.95831	20.18888	25.96827
6.00E+00	0.145	6.979066	13.47106	19.50997	25.12742
8.00E+00	0.139	6.729256	13.00568	18.85975	24.31989
1.00E+01	0.138	**6.657016**	12.87087	18.67107	24.08515
1.50E+01	0.140	6.737556	13.02117	18.88141	24.34682

Table (16): Gamma Protection Efficiency (GPE, %) of Molybdenum Sulphide with different thickness from Phy-X / Linear Attenuation Coefficients.

E, MeV	LAC, cm^{-1}	Thickness, cm			
		0.5	1	2	1.5
8.00E-02	6.475	**96.07406**	99.84587	99.99976	99.99395
1.00E-01	3.733	84.5313	97.60719	99.94274	99.62986
1.50E-01	1.581	54.6495	79.43332	95.77012	90.67291
2.00E-01	0.999	39.3095	63.16663	86.43303	77.64564
3.00E-01	0.639	27.36073	47.23536	72.15893	61.67215
4.00E-01	0.514	22.6445	40.16127	64.19327	53.71146
5.00E-01	0.446	20.00276	36.00442	59.04566	48.80531
6.00E-01	0.402	18.22349	33.12602	55.27871	45.3128

E, MeV	LAC, cm^{-1}	Thickness, cm			
		0.5	1	2	1.5
8.00E-01	0.345	15.8294	29.15309	49.80716	40.36773
1.00E+00	0.306	14.19673	26.37799	45.79799	36.82991
1.50E+00	0.248	11.67216	21.98193	39.13182	31.08833
2.00E+00	0.217	10.30163	19.54202	35.26513	27.8305
3.00E+00	0.187	8.915356	17.03588	31.16954	24.43242
4.00E+00	0.173	8.27669	15.86834	29.21864	22.83166
5.00E+00	0.166	7.958683	15.28396	28.23192	22.02624
6.00E+00	0.163	7.805646	15.00201	27.75342	21.63665
8.00E+00	0.161	**7.745381**	14.89085	27.56433	21.48288
1.00E+01	0.163	7.835509	15.05707	27.84698	21.71278
1.50E+01	0.172	8.224506	15.77259	29.05743	22.69988

Table (17): Gamma Protection Efficiency (GPE, %) of Stannous Sulphide with different thickness from Phy-X / Linear Attenuation Coefficients.

E, MeV	LAC, cm-1	Thickness, cm			
		0.5	1	1.5	2
1.00E-01	6.924	**96.86407**	99.90166	99.99692	99.9999
1.50E-01	2.599	72.73279	92.56499	97.97268	99.44721
2.00E-01	1.445	51.43481	76.41423	88.54552	94.43711
3.00E-01	0.773	32.06738	53.85159	68.65017	78.70324
4.00E-01	0.567	24.67701	43.26447	57.2651	67.8108
5.00E-01	0.470	20.9347	37.48679	50.57375	60.92099
6.00E-01	0.412	18.61821	33.77005	46.10088	56.13594
8.00E-01	0.343	15.76627	29.04679	40.23346	49.65642
1.00E+00	0.301	13.96552	25.98068	36.31786	45.2114
1.50E+00	0.242	11.38014	21.4652	30.40257	38.32285
2.00E+00	0.213	10.10514	19.18914	27.35519	34.69605
3.00E+00	0.188	8.95268	17.10385	24.52528	31.28229
4.00E+00	0.178	8.515722	16.30627	23.43339	29.95359
5.00E+00	0.175	8.365078	16.03041	23.05453	29.49108
6.00E+00	0.174	**8.348131**	15.99935	23.01183	29.43891
8.00E+00	0.178	8.511243	16.29807	23.42215	29.93988
1.00E+01	0.184	8.778734	16.78681	24.09187	30.75564
1.50E+01	0.200	9.506494	18.10925	25.89419	32.93906

Table (18): Gamma Protection Efficiency (GPE, %) of Stannic Sulphide with different thickness from Phy-X / Linear Attenuation Coefficients.

E, MeV	LAC, cm-1	Thickness, cm			
		0.5	1	1.5	2
1.00E-01	5.218	**92.63765**	99.45796	99.96009	99.99706
1.50E-01	2.017	63.52958	86.69908	95.1491	98.23086

E, MeV	LAC, cm-1	Thickness, cm			
		0.5	1	1.5	2
2.00E-01	1.158	43.9518	68.58599	82.39302	90.1316
3.00E-01	0.651	27.783	47.84706	62.33671	72.8007
4.00E-01	0.490	21.74081	38.75499	52.07015	62.49049
5.00E-01	0.412	18.63598	33.79896	46.13617	56.17423
6.00E-01	0.365	16.67842	30.57514	42.15411	51.80189
8.00E-01	0.307	14.21626	26.41149	36.87303	45.84732
1.00E+00	0.270	12.63075	23.66615	33.30769	41.73143
1.50E+00	0.217	10.30399	19.54626	27.83621	35.27196
2.00E+00	0.191	9.114033	17.39741	24.92584	31.76812
3.00E+00	0.166	7.980608	15.32431	22.08195	28.30028
4.00E+00	0.156	7.504385	14.44561	20.86594	26.80447
5.00E+00	0.152	7.299343	14.06588	20.33851	26.15327
6.00E+00	0.150	**7.226562**	13.93089	20.15073	25.92109
8.00E+00	0.151	7.27785	14.02603	20.28308	26.08476
1.00E+01	0.155	7.442081	14.33032	20.70592	26.60705
1.50E+01	0.166	7.955598	15.27828	22.0184	28.2223

Table (19): Gamma Protection Efficiency (GPE, %) of Zinc Sulphide with different thickness from Phy-X / Linear Attenuation Coefficients.

E, MeV	LAC, cm^{-1}	Thickness, cm			
		0.5	1	1.5	2
6.00E-02	5.372	**93.18524**	99.53559	99.96835	99.99784
8.00E-02	2.642	73.30706	92.87487	98.09809	99.49233
1.00E-01	1.635	55.85731	80.51423	91.39846	96.20305
1.50E-01	0.845	34.444	57.02411	71.82672	81.53073
2.00E-01	0.619	26.60191	46.1272	60.45839	70.97721
3.00E-01	0.460	20.5368	36.856	49.82376	60.12835
4.00E-01	0.392	17.78065	32.39978	44.41954	54.3021
5.00E-01	0.350	16.04679	29.51858	40.82859	50.3237
6.00E-01	0.320	14.78426	27.38277	38.11869	47.26738
8.00E-01	0.278	12.97673	24.26951	34.09685	42.64893
1.00E+00	0.249	11.6896	22.01273	31.12913	39.17986
1.50E+00	0.202	9.625036	18.32366	26.18504	33.28975
2.00E+00	0.177	8.452378	16.19033	23.27424	29.75939
3.00E+00	0.150	7.208096	13.89663	20.10304	25.86209
4.00E+00	0.136	6.593663	12.75256	18.50536	23.87885
5.00E+00	0.129	6.258972	12.1262	17.62619	22.78195
6.00E+00	0.125	6.072171	11.77563	17.13276	22.1646
8.00E+00	0.122	5.923181	11.49552	16.7378	21.66957
1.00E+01	0.122	**5.912656**	11.47572	16.70985	21.63451

E, MeV	LAC, cm^{-1}	Thickness, cm			
		0.5	1	1.5	2
1.50E+01	0.125	6.072651	11.77653	17.13403	22.16619

Table (20): Gamma Protection Efficiency (GPE, %) of the tested sulphides by NGCAL, x=0.5 cm.

Sample ID	GPE, %, x=0.5 cm				
	Neutrons		Photons		
	Thermal (25.4 meV)	Fast (4MeV)	0.1 MeV	1 MeV	15 MeV
Ag_2S	67.62391	1.029167	99.1116	19.45064	13.62311
As_2S_3	4.443262	0.059982	53.50149	9.836906	5.152514
CoS	53.54797	8.309371	58.97137	15.24878	7.609867
$CuFeS_2$	5.469722	0.646402	50.43821	11.7459	5.856503
FeS	5.630287	0.67223	52.74917	13.79138	6.737305
MoS_2	3.362179	0.049988	84.53669	14.19561	8.226812
SnS	1.192829	0.029996	96.85954	13.96362	9.507209
SnS_2	1.266906	0.024997	92.62998	12.62841	7.955681
ZnS	2.151517	0.104945	55.85542	11.68851	6.072784

Table (21): Gamma Protection Efficiency (GPE, %) of the tested sulphides by NGCAL, x=1 cm.

Sample ID	GPE, %, x=1 cm				
	Neutrons		Photons		
	Thermal (25.4 meV)	Fast (4MeV)	0.1 MeV	1 MeV	15 MeV
Ag_2S	89.51789	2.047743	99.99211	35.118	25.39033
As_2S_3	8.689098	0.119928	78.37889	18.70616	10.03954
CoS	78.42209	15.92828	83.16651	28.1723	14.64063
$CuFeS_2$	10.64027	1.288625	75.43629	22.11213	11.37002
FeS	10.94357	1.339942	77.67359	25.68074	13.0207

Sample ID	GPE, %, x=1 cm				
	Neutrons		Photons		
	Thermal (25.4 meV)	Fast (4MeV)	0.1 MeV	1 MeV	15 MeV
MoS_2	6.611316	0.09995	97.60886	26.37606	15.77682
SnS	2.371429	0.059982	99.90137	25.97742	18.11055
SnS_2	2.517762	0.049988	99.45683	23.66205	15.27843
ZnS	4.256745	0.20978	80.51256	22.01081	11.77678

Table (22): Gamma Protection Efficiency (GPE, %) of the tested sulphides by NGCAL, x=1.5 cm.

Sample ID	GPE, %, x=1.5 cm				
	Neutrons		Photons		
	Thermal (25.4 meV)	Fast (4MeV)	0.1 MeV	1 MeV	15 MeV
Ag_2S	96.6063	3.055836	99.99993	47.73797	35.55448
As_2S_3	12.74628	0.179838	89.94651	26.70296	14.67477
CoS	89.97662	22.91412	93.09345	39.12515	21.13637
$CuFeS_2$	15.52799	1.926697	87.82579	31.26076	16.56064
FeS	15.9577	2.003165	89.45059	35.93039	18.88076
MoS_2	9.75121	0.149888	99.63025	36.82743	22.7057
SnS	3.535971	0.08996	99.9969	36.31365	25.89595
SnS_2	3.752771	0.074972	99.95997	33.30232	22.01861
ZnS	6.316677	0.314504	91.39735	31.12659	17.13439

Table (23): Gamma Protection Efficiency (GPE, %) of the tested sulphides by NGCAL, x=2 cm.

Sample ID	GPE, %, x=2 cm				
	Neutrons		Photons		
	Thermal (25.4 meV)	Fast (4MeV)	0.1 MeV	1 MeV	15 MeV
Ag_2S	98.90125	4.053554	100	57.90326	44.33396
As_2S_3	16.62319	0.239712	95.32528	33.91312	19.07117

Sample ID	GPE, %, x=2 cm				
	Neutrons		Photons		
	Thermal (25.4 meV)	Fast (4MeV)	0.1 MeV	1 MeV	15 MeV
CoS	95.34394	29.31947	97.16634	48.40782	27.13779
$CuFeS_2$	20.14838	2.560645	93.96624	39.3348	21.44726
FeS	20.68953	2.661929	95.01532	44.76647	24.34601
MoS_2	12.78554	0.1998	99.94282	45.79516	29.06456
SnS	4.686621	0.119928	99.9999	45.20658	32.94118
SnS_2	4.972133	0.09995	99.99705	41.72517	28.22256
ZnS	8.33229	0.419119	96.2024	39.17687	22.16664

5. Conclusions

Various metal sulphides were selected for gamma and neutron shielding prediction by two online models (Phy-X and NGCAL). The gamma parameters calculated by both software programs in the studied energy range were found to be identical according to the differences ($\Delta\% < 1\%$) between both models.

The Mass Attenuation Coefficient (MAC) was calculated by both software programs, and the resulting values decreased with increasing incident energy depending on photon or neutron interactions with the material. For thermal neutrons (25.4 meV) or fast neutrons (4 MeV), the MAC showed that Ag_2S or CoS was a superior neutron attenuator. According to the NGCAL model, MAC and LAC presented Ag_2S as a superior photon attenuator, especially at 15 MeV.

According to the Phy-X model, the highest MAC value was found for Ag_2S in all tested energy ranges because it contains two silver ions with the highest density, mean atomic number, and metal composition in addition to the lowest (S%) among all sulphides under evaluation. Additionally, Ag_2S has a monoclinic structure and two silver ions linked to one sulphide ion. From the crystal lattice data, it can be concluded that the presence of heavy packed ions in the unit cell resulted in more gamma attenuation. By Phy-X estimation of the monosulphides and disulphides, the MAC increased with increasing mean atomic number and metal content. It can be concluded that more metal ion packing or volume may lead to an increase in gamma attenuation.

The Mean Free Path (MFP) values were also calculated by both mathematical models and showed that Ag_2S had the greatest effect on all tested incident energies because of its quick interaction with the photon source compared to the other tested sulphides.

In general, the lower half value layer (HVL) presents excellent gamma shielding depending on the chemical composition, while the energy influence becomes more effective at > 0.1 MeV due to the photoelectric mechanism. At the highest incident energy (15 MeV), the HVL increasing sequence according to the Phy-X model was **Ag_2S**, SnS, MoS_2, SnS_2, CoS, FeS, ZnS, $CuFeS_2$, and **As_2S_3**. The HVL values at (0.1, 1, and 15) MeV, calculated by the NGCAL model, showed various increasing trends at incidence, where the HVL sequence at (0.1, 1, 15) MeV according to both models presented 100% similarity considering that silver sulphide was the best material for gamma shielding.

The TVL of all tested materials was calculated by NGCAL, and the increasing sequence of TVL was found to be identical to that of HVL at 1 MeV and 15 MeV because HVL and TVL mainly depend on LAC data.

The Effective Atomic Number Z_{eff} variation with the energy range (0.015–15 MeV) was also estimated by the Phy-X model, which may be associated with the density, mean atomic number, composition (%) or weight

fraction, total atomic cross-section, crystal geometry and elemental packing of each molecule. From the obtained Z_{eff} data, it can be concluded that Ag_2S was the superior attenuator between the sulphides under prediction, especially at higher energies.

The Gamma Protection Efficiency (GPE, %) was also calculated as a calculated parameter for the gamma shielding subject based on the linear attenuation coefficient (LAC) data presented in the Beer–Lamberts law: $GPE\% = (1 - (e^{-\mu x}) * 100$, where the thickness (x) was assumed. In this study, the GPE% for gamma shielding increased with increasing thickness and decreased with increasing energy. Additionally, silver sulphide showed the highest GPE among the other tested materials. The GPE% of the thermal or fast neutrons was also calculated, where the increasing order was **SnS, SnS_2, ZnS, MoS_2, As_2S_3, $CuFeS_2$, FeS, CoS, and Ag_2S** for thermal neutrons and **SnS_2, SnS, MoS_2, As_2S_3, ZnS, $CuFeS_2$, FeS, Ag_2S, and CoS** for fast neutrons.

Conflict of Interest: The authors declare that there are no conflicts of interest associated with this research project. We have no financial or personal relationships that could potentially bias our work or influence the interpretation of the results.

References

[1] N. Tsoulfanidis and S. Landsberger, "Measurement and Detection of Radiation", CRC Press, USA, 2021.

[2] A. Acevedo-Del-Castillo, E. Águila-Toledo, S. Maldonado-Magnere, and H. Aguilar-Bolados, "A Brief Review on the High-Energy Electromagnetic Radiation-Shielding Materials Based on Polymer Nanocomposites." *International journal of molecular sciences*, vol. 22, no. 16, pp. 9079, 2021.

[3] C. More, Z. Alsayed, M. Badawi, A. Thabet, and P. Pawar, "Polymeric composite materials for radiation shielding: a review." *Environmental Chemistry Letters*, vol. 19, no.3, pp. 2057–2090, 2021.

[4] B. Subedi, J. Paudel, and T. Lamichhane, "Gamma-ray, fast neutron and ion shielding characteristics of low-density and high-entropy Mg-Al-Ti-V-Cr-Fe-Zr-Nb alloy systems using Phy-X/PSD and SRIM programs," *Heliyon*, vol. 9, no. 7, article number: e17725, 2023.

[5] C. Kursun, M. Gao, S. Guclu, Y. Gaylan, K. Parrey, and A. Yalcin, "Measurement on the neutron and gamma radiation shielding performance of boron-doped titanium alloy $Ti_{50}Cu_{30}Zr_{15}B_5$ via arc melting technique," *Heliyon*, vol. 9, no. 11, article number: e21696, 2023.

[6] I. Nabil, M. El-Samrah, A. Omar, A. Tawfic, and A. El Sayed, "Experimental, analytical, and simulation studies of modified concrete mix for radiation shielding in a mixed radiation field," *Scientific reports*, vol. 13, no. 1, pp. 17637, 2023.

[7] G. Lakshminarayana, Y. Elmahroug, A. Kumar, H. Tekin, N. Rekik, M. Dong, D. Lee, J. Yoon, and T. Park, "Detailed Inspection of γ-ray, Fast and Thermal Neutrons Shielding Competence of Calcium Oxide or Strontium Oxide Comprising Bismuth Borate Glasses," *Materials (Basel, Switzerland)*, vol. 14, no. 9, pp. 2265, 2021.

[8] M. Almatari, S. Issa, M. Dong, M. Sayyed, and R. Ayad, "Comparison between MCNP5, Geant4 and experimental data for gamma rays attenuation of PbO-BaO-B_2O_3 glasses." *Heliyon*, vol. 5, no. 8, article number: e02364, 2019.

[9] Y.Wu, Y. Cao, Y. Wu, and D. Li, "Mechanical Properties and Gamma-Ray Shielding Performance of 3D-Printed Poly-Ether-Ether-Ketone/Tungsten Composites," *Materials (Basel, Switzerland)*, vol. 13, no. 20, pp. 4475, 2020.

[10] H. Tekin, S. Issa, G. Kilic, H. Zakaly, M. Abuzaid, N. Tarhan, K. Alshammari, H. Sidek, K. Matori, and M. Zaid, "In-Silico Monte Carlo Simulation Trials for Investigation of V_2O_5 Reinforcement Effect on Ternary Zinc Borate Glasses: Nuclear Radiation Shielding Dynamics. *Materials (Basel, Switzerland)*, vol. 14, no. 5, pp. 1158. 2021.

[11] F. Huang, Y. Wang, P. Wang, H. Ma, X., Chen, K. Cao, Y. Pei, J. Peng, J. Li, and M. Zhai, "Oxidized multiwall carbon nanotube/silicone foam composites with effective electromagnetic interference shielding and high gamma radiation stability," *RSC Advances*, vol. 8, no. 43, pp. 24236–24242, 2018.

[12] J. Wang, H. Zhou, Y. Gao, Y. Xie, J. Zhang, Y. Hu, D. Wang, Z. You, S. Wang, H. Li, G. Liu, and A. Mi, "The Characterization of Silicone-Tungsten-Based Composites as Flexible Gamma-Ray Shields." *Materials (Basel, Switzerland)*, vol. 14, no. 20, pp. 5970, 2021.

[13] X. Yang, D. Salado-Leza, E. Porcel, C. González-Vargas, F. Savina, D. Dragoe, H. Remita, and s. Lacombe, "A Facile One-Pot Synthesis of Versatile PEGylated Platinum Nanoflowers and Their

Application in Radiation Therapy," *International Journal of Molecular Sciences*, vol. 21, no. 5, pp. 1619, 2020.

[14] D. Toyen, Y. Paopun, D. Changjan, E. Wimolmala, S. Mahathanabodee, T. Pianpanit, T. Anekratmontree, and K. Saenboonruang, Simulation of Neutron/Self-Emitted Gamma Attenuation and Effects of Silane Surface Treatment on Mechanical and Wear Resistance Properties of Sm_2O_3/UHMWPE Composites," *Polymers*, vol. 13, no. 19, pp. 3390, 2021.

[15] C. Ma, H. Liu, H. Wolterbeek, A. Denkova, and P. Serra Crespo, "Effects of High Gamma Doses on the Structural Stability of Metal-Organic Frameworks." *Langmuir: The ACS Journal of Surfaces and Colloids*, vol. 38, no. 29, pp. 8928–8933, 2022.

[16] H. Gökçe, O. Güngörb, and H. Yılmaz An online software to simulate the shielding properties of materials for neutrons and photons: NGCal," Radiation Physics and Chemistry, vol. 185, article number 109519, 2021.

[17] F. Al-Saeedi, H. Alsafi, O. Tahlykov, M. Sayyed, H. Al Ghamdi, E. Kolobkova, F. Kapustin, A. Almuqrin, and K. Mahmoud, "Fabrication, characterization, and gamma-ray shielding performance for the lead-based Iraqi white silicate glasses: A closer examination," Opik, vol. 260, article number 169103, 2022.

[18] A. Sameer and A. Ali, "Gamma-Ray Shielding Effectiveness of Clay and Boron Doped Clay Material at Different Thicknesses," *Iraqi Journal of Science*, vol. 63, no. 5, pp. 1961-1970, 2022.

[19] A. Shareef and A. Kadim, "Effect of Barium Sulfate Nanoparticles with Organic Alcohol on the Ionizing Radiation Shielding," *Iraqi Journal of Science*, vol. 64, no. 7, pp. 3356-3361, 2023.

[20] B. Ghafoor and Y. Shawn, "Investigate shielding of standard materials and glass for stopping 662 KeV gamma ray penetrations," *Tikrit Journal of Pure Science*, vol. 28, no. 2, pp. 83-87, 2023..

[21] S. Mahmood, A. Aobiad, and M. Mutter, "Synthesis and Characterization of PMMA/Bi_2O_3-Fe_2O_3 Composites as Gamma Radiation Shielding," *Sumer Journal for Pure Science*, vol. 2, no. 2, pp. 120-133, 2023.

[22] A. El-Sawy and E. Sarwat, "Comparative Study of Gamma- Ray Shielding Parameters for Different Epoxy Composites," *Baghdad Science Journal*, vol. 21, no. 2, pp. 0480-0495, 2024.

[23] N. Ekinci, K. Mahmoud, B. Aygun, M. Hessien, and Y. Rammah, "Impacts of the colemanite on the enhancementof the radiation shielding capacity of polypropylene," *Journal of Materials Science: Materials in Electronics*, vol. 33, no. 3, pp. 20046-20055, 2022.

[24] G. Mahmoud, M. Sayyed, A. Almuqrin, J. Arayro, and Y. Maghrbi, "Monte Carlo Investigation of Gamma Radiation Shielding Features for Bi_2O_3/Epoxy Composites" *Applied Sciences* vol. 13, no. 3, article number 1757, 2023.

[25] K. Alsafi, D. Aloraini, M. Saif, and K. Shaaban, "Gamma and neutron attenuation of SiO_2–B_2O_3–BaO–Li_2O glasses doped with CeO_2" *Radiochimica Acta*, 2024.

[26] G. Hiremath, V. Singh, N. Ayachit, and N. Badiger, "Study of gamma, neutron, and proton interaction parameters of some immunotherapy drugs using EpiXs, NGCal, and PSTAR software" *Radiochimica Acta*, 2024.

[27] Y. Le, J. She, J. Mao, X. Jing, J. Yang, X. Meng, J. Tan, L. Wu, W. Zhang, W. Yang, X. Pang, and F. Pan, "Novel integrated structure and function of Mg–Gd neutron shielding materials" *Nanotechnology Reviews*, vol. 13, no. 1, pp. 20240007, 2024.

[28] J. Winiecki, "Principles of radiation therapy" Physical Sciences Reviews, vol. 7, no. 12, pp. 1501-1528, 2022.